Force dependence of filopodia adhesion: involvement of myosin II and formins

N.O. Alieva[1]†, A.K. Efremov[1,2]†, S. Hu[1], D. Oh[1], Z. Chen[1], M. Natarajan[1], H.T. Ong[1], A. Jégou[3], G. Romet-Lemonne[3], J.T. Groves[1,4], M.P. Sheetz[1,5], J. Yan[1,2,6], A.D. Bershadsky[1,7]*

Affiliations:

[1]Mechanobiology Institute, National University of Singapore, T-lab, 5A Engineering Drive 1, Singapore 117411, Singapore.

[2]Center for BioImaging Sciences, National University of Singapore, 14 Science Drive 4, Singapore 117557, Singapore.

[3]Institut Jacques Monod, 15 rue Helene Brion 75205 Paris cedex 13, France.

[4]Department of Chemistry, University of California, Berkeley, CA, 94720, USA.

[5]Department of Biological Sciences, Columbia University, New York, New York 10027, USA.

[6]Department of Physics, National University of Singapore, Singapore 117542, Singapore

[7]Weizmann Institute of Science, Herzl St 234, Rehovot, 7610001, Israel

*Correspondence to: alexander.bershadsky@weizmann.ac.il.

† Equal contribution.

Abstract: Filopodia are dynamic membrane protrusions driven by polymerization of an actin filament core, mediated by formin molecules at the filopodia tips. Filopodia can adhere to the extracellular matrix and experience both external and cell generated pulling forces. The role of such forces in filopodia adhesion is however insufficiently understood. Here, we induced sustained growth of filopodia by applying pulling force to their tips via attached fibronectin-coated beads trapped by optical tweezers. Strikingly, pharmacological inhibition or knockdown of myosin IIA, which localized to the base of filopodia, resulted in weakening of filopodia adherence strength. Inhibition of formins, which caused detachment of actin filaments from formin molecules, produced similar effect. Thus, myosin IIA-generated centripetal force transmitted to the filopodia tips through interactions between formins and actin filaments is required for filopodia adhesion. Force-dependent adhesion led to preferential attachment of filopodia to rigid versus fluid substrates, which may underlie cell orientation and polarization.

Filopodia are ubiquitous cell extensions involved in cell motility, exploration of the microenvironment and adhesion [1, 2]. These finger-like membrane protrusions help cells to determine the direction of movement [3], establish contacts with other cells [4, 5] and capture inert particles or living objects (bacteria), which cells subsequently engulf [6-9]. Filopodia are involved in numerous processes of embryonic development, as well as in cell migration in adult organisms. Moreover, augmented filopodia activity is a hallmark of tumor cells, which use them in the processes of invasion and metastasis [1].

The main element of filopodia is the actin core, which consists of parallel actin filaments with barbed ends oriented towards the tip, and pointed ends toward the cell

body [1, 2, 10]. Actin filaments are connected to each other by several types of crosslinking proteins [11-14]. The filopodia grow via actin polymerization at the tip, in a process driven by formin family proteins such as mDia2 [15-17], FMNL2 & 3 [18-20], as well as by actin elongation protein Ena/VASP [15, 21, 22]. In addition to proteins that crosslink and polymerize actin, filopodia also contain actin based molecular motors, such as myosin X localized to the tip of the filopodia. Although the function of myosin X is unclear, it is known to be required for filopodia growth, and its overexpression promotes filopodia formation [23, 24].

Adhesion of the filopodia to the extracellular matrix (ECM) is mediated by the integrin family of receptors (e.g. $\alpha_v\beta_3$) [25, 26], which are localized to the tip area. One possible function of myosin X is the delivery of integrins to this location [25]. In addition to integrins, filopodia tips have been shown to contain other proteins involved in integrin mediated adhesion, such as talin and RIAM [27]. Several studies suggest that typical cell matrix adhesions, known as focal adhesions, could in some cases originate from filopodia [28, 29]. Thus, filopodia could be considered primary minimal cell matrix adhesion structures.

The hallmark of integrin mediated adhesions of focal adhesion type is their mechanosensitivity [30-32]. They grow in response to pulling forces applied to them, either by the actomyosin cytoskeleton, or exogenously by micromanipulations and may play a role in matrix rigidity sensing. Indeed, correlation between focal adhesion size and matrix rigidity is well documented [33-35]. Filopodia also may participate in matrix rigidity sensing. For example, it was demonstrated that cell durotaxis, a preferential cell movement along a gradient of substrate rigidity is mediated by

filopodia [36]. However, force dependence of filopodia adhesion has not yet been explored.

In the present study, we monitored filopodia adhesion and growth under conditions of pulling with a constant rate. We have demonstrated that adhesion of filopodia to the ECM strongly depends on myosin II activity and found myosin II filaments localized to the base of filopodium. Moreover, formin family protein activity at the filopodia tips is also required for filopodia adhesions, most probably through a role in the transmission of force through the actin core, from the filopodium base to the filopodium tip. Thus, filopodia are elementary units demonstrating adhesion dependent mechanosensitivity.

RESULTS

Dynamics of filopodia induced by expression of myosin X in HeLa-JW cells

Transfection of HeLa-JW cells with either GFP-myosin X or mApple-myosin X resulted in a strong enhancement of filopodia formation in agreement with previous studies [37]. During filopodia movement, myosin X was concentrated at the filopodia tips, forming characteristic patches sometimes also called “puncta” or “comet tails” (fig. S1A, movie S1). Here, we focused on filopodia originating from stable cell edges and extending along the fibronectin-coated substrate. These filopodia demonstrated apparent dynamic instability, where periods of persistent growth, with an average velocity of 67 ± 6 nm/s (mean ± SEM, n = 89), were interrupted by pauses and periods of shrinking with an average velocity of 28 ± 3 nm/s (mean ± SEM, n = 100). This behavior is consistent with previously published results [38]. In addition to myosin

X, the filopodia tips were also enriched in several other proteins such as mDia2, VASP and talin (fig. S1B).

To observe the dynamics of filopodia adhesion and protrusion under controlled experimental conditions, we monitored the growth of filopodia that were adhered to fibronectin-coated beads trapped by optical tweezers. First, 2μm diameter fibronectin-coated polystyrene beads were placed onto filopodia tips by the optical tweezers. After 20-30 s, which is required for the initial attachment of the bead to the filopodium, the movement of microscope piezo stage, in the direction from the tip to base of filopodium, was initiated (Fig. 1, movie S2). The force exerted by filopodium on the bead was monitored by measuring the bead displacement from the center of the trap (Δx). In order to preserve the structural integrity of the filopodia, the velocity of the stage movement was set to approximately 10-20nm/s, which is slower than the average velocity of spontaneous filopodia growth. With this setup we observed sustained filopodia growth for more than 10 mins, during which time the tdTomato-Ftractin labelled actin core remained intact (Fig. 1B). Pulling-induced filopodia growth depended on integrin mediated adhesion of filopodia tips to fibronectin-coated beads. When the beads were coated with concanavalin A instead of fibronectin, application of force usually resulted in the formation of membrane tethers, rather than growth of the filopodia (movie S3).

During the first 3 mins after stage movement commenced, the exerted force approached the maximal value of 3-5 pN. However, it then dropped to the 1.5-2pN range, and remained at this level for a further 1-3 mins, after which it rapidly increased again (Fig. 1C). In a typical experiment, we detected ~ 5 such peaks with a

mean peak force value of 3pN alternating with the 1-3 min periods of lower force (1.5-2pN).

Immediately after attachment of the bead to the filopodium tip, the myosin X patch, or a significant portion that pinched off the main myosin X mass, started to move centripetally with an approximate velocity of 31 ± 5 nm/s (mean ± SEM, n = 42) (fig. S2A). Experiments where myosin X and VASP were co-expressed revealed that the retrograde movement of myosin X patches colocalized with the patches of VASP (fig. S1B middle & fig. S6). However myosin X did not entirely disappear from the filopodium tip and the original amount was fully restored after several minutes (Fig. 1C, kymograph), even though detachment and subsequent centripetal movement of myosin X portions from the filopodium tip were occasionally observed throughout the entire period of force-induced filopodium growth (movie S2).

Effects of myosin II inhibition

Expression of GFP labeled myosin light chain in HeLa-JW cells showed that myosin II does not localize to the filopodia tips or shafts, but is often located at the proximal ends of the filopodia (Fig. 2A). Structure illumination microscopy (SIM) revealed few myosin II mini-filaments either side of the filopodium base. We further studied how the presence and activity of myosin II affects unconstrained and force-induced filopodia growth.

The function of myosin II was suppressed in three separate experiments; through the inhibition of ROCK by Y27632, by siRNA mediated knockdown of myosin IIA heavy chain (MYH9), and through the inhibition of myosin II ATPase activity by

light-insensitive S-nitro-blebbistatin. Inhibition of ROCK blocks myosin II regulatory light chain (RLC) phosphorylation, which interferes with myosin II filament assembly [39-42]. As a result, cells treated with Y27632 essentially lose their myosin II filaments (Fig. 2B, movie S4). siRNA knockdown of MYH9 also resulted in a loss of most of the myosin II filaments (fig. S3). Inhibition of myosin II ATPase activity by S-nitro-blebbistatin did not disrupt myosin II filaments [42], although this treatment did result in profound changes to the organization of the actomyosin cytoskeleton, including a loss of stress fibers. Myosin IIA knockdown or myosin II inhibition resulted in disappearance of long (>10μm) filopodia, but changed the average filopodia length only slightly (Fig. 2C). Myosin X positive comet tails persisted at the tips of filopodia in the treated cells (Fig. 2B).

Despite the morphological integrity of filopodia being preserved in myosin II inhibited or depleted cells, adhesion of filopodia to the ECM was significantly impaired. While in control cells application of pulling force via fibronectin-coated bead induced sustained growth of attached filopodia accompanied by the development of up to ~ 5 pN force, in the cells with impaired myosin II activity the filopodia detached earlier, after developing rather small forces (Fig. 3B-C, E, movie S5B-C). This suggests the filopodia are unable to establish a proper adhesion contact in the absence of active myosin II. We also examined the immediate effect of Y27632 during the force-induced sustained growth of filopodia. After the drug was added, filopodia detached from the bead (fig. S4, movie S6).

Interaction between actin filaments and formins is required for filopodia adhesion and myosin X localization

In myosin X-induced filopodia, the formin mDia2 is localized to the filopodia tip, and overlaps with myosin X patches (fig. S1B). Small molecular inhibitor of formin homology domain 2 (SMIFH2) [43] was used to investigate the role of formins in attachment of filopodia to fibronectin-coated beads. We found that in SMIFH2 (40μM, 1hour) treated cells, adhesion of filopodia to the beads was impaired in a similar way to the adhesion of filopodia in myosin II inhibited/depleted cells. The duration of contact between the filopodia and the bead was significantly shorter, and the maximal force exerted by filopodia to the bead was significantly weaker than in control cells (Fig. 3D-E, movie S5D).

While the number of filopodia in cells treated with SMIFH2 remained the same as in control cells and their mean length decreased only slightly (Figs. 3D and 4A, fig. S5), practically none of these filopodia had myosin X comet tails at their tips (Fig. 3D and fig. S5) despite originally being induced by over-expression of myosin X. We found that SMIFH2 induced rapid disintegration of the comet tails into myosin X patches, which rapidly moved centripetally towards the cell body (Fig. 4B, movie S7). Although such movement was occasionally observed in control cells (see above and fig. S2A), it was much more prominent in cells treated with SMIFH2 (fig. S2B), and led to the apparent disappearance of myosin X from the filopodia tips. Of note, the movement of myosin X patches in SMIFH2 treated cells occurred together with the movement of its partner VASP [44], another protein associated with barbed ends of actin filaments (fig. S6).

The velocity of retrograde movement of myosin X patches in filopodia of cells treated with SMIFH2 was 84 ± 22 nm/s (mean ± SEM, n = 45) (fig. S2B). This is higher than

the estimated velocity of actin treadmilling in filopodia, which is reported to be 10-20nm/s [37]. We therefore hypothesized that such movement results from the detachment of myosin X-bearing actin filaments from the filopodia tips. Once free, their subsequent retrograde movement is driven by myosin II located at the bases of the filopodia. Indeed, incubation of SMIFH2 treated cells with Y27632 efficiently stopped the retrograde movement of the myosin X positive patches (Fig. 4C, movies S8A-C).

To prove that SMIFH2 treatment can detach actin filaments from formin located at the filopodia tip, we performed in vitro experiments where the actin filaments were growing from immobilized formin mDia1 construct (FH1FH2DAD) in the absence or presence of SMIFH2. Following treatment with 100μM SMIFH2, a rapid decrease in the fraction of filaments remaining associated with immobilized formin under conditions of mild shear flow ("survival fraction") was observed (fig. S7). Thus, SMIFH2 treatment disrupted physical contacts between formin molecules and actin filaments. Therefore, SMIFH2-induced rapid centripetal movement of myosin X is driven by myosin II mediated pulling of actin filaments detached from the filopodia tips.

Effect of myosin II and formin inhibition on the growth of unconstrained filopodia

In addition to the studies of filopodia growing in response to pulling forces, we examined the effects of myosin II and formin inhibition on the dynamics of free, unconstrained filopodia (Fig. 5 inset). We found that knockdown of myosin IIA and cell treatment with Y27632 or S-nitro-blebbistatin efficiently blocked growth and

retraction of unconstrained filopodia, resulting in suppression of filopodia dynamics. In untreated myosin X expressing cells, the fraction of filopodia in the "pause" state (with the growth rate between -15 and +15nm/s) was 13% (n = 194). At the same time, fractions of the "pausing" filopodia were 90% (n = 41), 80% (n = 83) and 55% (n = 42) for myosin IIA knockdown, S-nitro-blebbistatin-treated and Y27632-treated cells, respectively (Fig. 5). Similarly, the fraction of "pausing" filopodia in cells treated with the formin inhibitor SMIFH2 was 75% (n = 44) (Fig. 5B).

DISCUSSION

In this study, we have shown that filopodia adhesion to the ECM is a force dependent process. This conclusion is based on experiments in which sustained growth of filopodia was maintained by the application of pulling force at the interface between a fibronectin-coated bead, and the tip of a filopodia. With this setup, inhibition of myosin II filament formation or myosin II ATPase activity resulted in suppression of filopodia adhesion to fibronectin-coated bead. Our experiments were performed on filopodia induced by over-expressing myosin X and, therefore, our conclusions are, strictly speaking, only valid for this class of filopodia. However, myosin X has been shown to be a universal component of filopodia [23], so employment of such an experimental system does not restrict the generality of our finding.

Since myosin II is located at the bases of filopodia (Fig. 2A-B), a question requiring clarification is how the pulling force is transmitted to the tips of the filopodia involved in adhesion. Our data are consistent with the idea that filaments of the actin core transmit the force generated through their interaction with myosin II to the filopodium tip. We have shown that formin inhibition by SMIFH2 suppresses

filopodia adhesion to the beads in the same manner as inhibition of myosin II. Moreover, we demonstrated that SMIFH2 treatment led to a rapid, myosin II-dependent, movement of actin filament associated proteins, myosin X and VASP, from the filopodia tip towards the cell body. We interpret such movements as evidence of actin filament detachment from formins at the filopodia tips in the cells treated with SMIFH2. Indeed, *in vitro* experiments demonstrated that addition of SMIFH2 to actin filaments growing from the immobilized formin under a condition of moderate flow results in the detachment of actin filaments from the formin molecules. Together, these experiments suggest that myosin II inhibition, or the inhibition of the formin-mediated association between actin filaments and the filopodia tips, makes filopodia unable to form stable adhesions with fibronectin-coated beads. This in turn prevents them from growing upon force application.

To check whether adhesion and growth of filopodia require the pulling force, we compared behavior of unconstrained filopodia on rigid substrate with that on fluid supported lipid bilayer (SLB) where the traction forces cannot develop [45]. To this end, we created a composite substrate on which rigid surface was covered by orderly patterned small islands (D = 3μm) of SLB. Both rigid and fluid areas were coated with integrin ligand RGD peptide with the same density (fig. S8). We found that dynamics of filopodia extended over rigid regions of this substrate was similar to that of filopodia growing on rigid fibronectin-coated substrate used in previous experiments. At the same time, filopodia that encountered the SLB islands could not attach properly and as a result spent over such substrate significantly shorter time than over rigid area of the same geometry (Fig. 6A, B). Accordingly, the average density of filopodia tips remaining inside the SLB islands during period of observation (>

10min) was lower than that on the rigid substrate (Fig. 6C). Thus, not only inhibition of myosin II or formin, but also micro-environmental conditions under which filopodia tips do not develop traction force, prevent proper adhesion of filopodia.

In the present study, we have demonstrated that adhesion of filopodia tips depends on myosin II filament formation and activity. We found few individual myosin II filaments at the base of many filopodia. The force generated by one bipolar myosin IIA filament (consisting of about 30 individual myosin molecules [46], 15 at each side) can be estimated based on the stall force for individual myosin IIA molecule (3.4pN according [47]) and duty ratio (5-11% according [48]) as 2.6-5.6pN. This value is consistent with pulling forces generated by filopodium as measured in our experiments. The myosin II-driven force is transmitted to the filopodium tip via actin core associated with formin molecules at the tip. Such force appears to be sufficient to overcome the actin filament crosslinking inside the core, which can explain the fast retrograde translocation of some of core filaments (together with associated myosin X and VASP) upon treatment with formin inhibitor that detaches the actin filaments from formin.

Force-dependent growth of filopodia is an integrin-dependent process and was not observed in experiments with integrin-independent adhesion of filopodia to beads coated by concanavalin A. A major link between integrin and actin filaments, talin, has been detected at the filopodia tips in this and other publications [27]. It was established that force-driven unfolding of talin facilitates interaction of talin with another adhesion complex component, vinculin, resulting in reinforcement of the association between talin and actin filaments [49-51]. Applicability of this mechanism to

filopodia adhesion reinforcement requires additional studies. While vinculin was detected in some filopodia [52], a RIAM protein that compete with vinculin for talin-binding in a force-dependent manner [27, 53] may also be involved. RIAM binds Ena/VASP and profilin [54] and could recruit these actin polymerization-promoting proteins to the filopodia tips.

Another mechanism of myosin II-dependence of filopodia adhesion and growth might involve formin-driven actin polymerization known to be a major factor in filopodia extension [15-20]. Recent studies demonstrate that formin-driven actin polymerization can be enhanced by pulling forces [55-58]. Thus, myosin II-generated force transmitted via actin core to formins at the filopodium tip can stimulate actin polymerization, promoting filopodia growth. Polymerization of actin could also be important for recruitment of new adhesion components to the filopodia tips and adhesion reinforcement [59].

Filopodia adhesion is tightly associated with filopodia growth and shrinking. In our experiments, inhibition of myosin II and formins not only suppressed filopodia adhesion but also resulted in reduction of motility of filopodia along the substrate. During pulling-induced growth of bead-attached filopodia, periods of filopodia elongation alternate with periods of growth cessation accompanied by increase of the pulling force. Thus, force developed during growth cessation may trigger the subsequent filopodia growth. Similarly, the growth of unconstrained filopodia along rigid substrate can proceed via periods of attachment, development of force, and consequent filopodia elongation [38]. Inhibition of force generation or transmission suppresses such dynamics.

Our finding that filopodia adhesion and growth is force-dependent explains how filopodia could respond differently to substrates of varying stiffness. On a stiff substrate, the force generated by myosin II and applied to the adhesion complex will develop faster than on a compliant substrate [60]. Accordingly, filopodia adhesion should be more efficient on stiff substrates than on compliant substrates. Moreover, integrin ligands associated with a substrate, which does not allow the development of pulling force, cannot fully support filopodia adhesion and growth. Indeed, we showed that the contacts of filopodia with RGD ligands associated with fluid membrane bilayer were shorter and less stable than with the areas of rigid substrate covered with RGD of the same density. These considerations can explain involvement of filopodia in the phenomenon of durotaxis [36], a preferential cell movement towards stiffer substrates [61]. This may provide a mechanism to rectify directional cell migration.

Orientation based on filopodia adhesion is characteristic for several cell types, in particular for nerve cells. The growth cones of most neurites produce numerous filopodia, and the adhesion of these filopodia can determine the direction of neurite growth [62, 63]. Interestingly, the filopodial-mediated traction force in growth cones is myosin II-dependent [64] and application of external force can regulate the direction of growth cone advance [65]. The results from these experiments can now be explained by preferential adhesion/growth of filopodia, which experience larger force. The mechanosensitivity of filopodia adhesion provides a mechanism of cell orientation that complements that mediated by focal adhesions. Focal adhesions are formed by cells attached to rigid two-dimensional substrates, whereas filopodia adhesion can be formed by cells embedded in three-dimensional fibrillar ECM network. Thus, further

investigation of filopodia mechanosensitivity could shed a new light on a variety of processes related to tissue morphogenesis.

1. G. Jacquemet, H. Hamidi, J. Ivaska, Filopodia in cell adhesion, 3D migration and cancer cell invasion. *Curr Opin Cell Biol* **36**, 23-31 (2015).
2. P. K. Mattila, P. Lappalainen, Filopodia: molecular architecture and cellular functions. *Nat Rev Mol Cell Biol* **9**, 446-454 (2008).
3. C. A. Heckman, H. K. Plummer, 3rd, Filopodia as sensors. *Cell Signal* **25**, 2298-2311 (2013).
4. P. J. Bryant, Filopodia: fickle fingers of cell fate? *Curr Biol* **9**, R655-657 (1999).
5. F. Prols, Sagar, M. Scaal, Signaling filopodia in vertebrate embryonic development. *Cell Mol Life Sci* **73**, 961-974 (2016).
6. S. Romero *et al.*, Filopodium retraction is controlled by adhesion to its tip. *J Cell Sci* **125**, 4999-5004 (2012).
7. L. Vonna, A. Wiedemann, M. Aepfelbacher, E. Sackmann, Micromechanics of filopodia mediated capture of pathogens by macrophages. *Eur Biophys J* **36**, 145-151 (2007).
8. J. Moller, T. Luhmann, M. Chabria, H. Hall, V. Vogel, Macrophages lift off surface-bound bacteria using a filopodium-lamellipodium hook-and-shovel mechanism. *Sci Rep* **3**, 2884 (2013).
9. T. Bornschlogl *et al.*, Filopodial retraction force is generated by cortical actin dynamics and controlled by reversible tethering at the tip. *Proc Natl Acad Sci U S A* **110**, 18928-18933 (2013).
10. J. Faix, D. Breitsprecher, T. E. Stradal, K. Rottner, Filopodia: Complex models for simple rods. *Int J Biochem Cell Biol* **41**, 1656-1664 (2009).
11. R. Jaiswal *et al.*, The formin Daam1 and fascin directly collaborate to promote filopodia formation. *Curr Biol* **23**, 1373-1379 (2013).
12. D. Vignjevic *et al.*, Role of fascin in filopodial protrusion. *J Cell Biol* **174**, 863-875 (2006).
13. V. Delanote *et al.*, An alpaca single-domain antibody blocks filopodia formation by obstructing L-plastin-mediated F-actin bundling. *FASEB J* **24**, 105-118 (2010).
14. I. Van Audenhove *et al.*, Fascin Rigidity and L-plastin Flexibility Cooperate in Cancer Cell Invadopodia and Filopodia. *J Biol Chem* **291**, 9148-9160 (2016).
15. M. Barzik, L. M. McClain, S. L. Gupton, F. B. Gertler, Ena/VASP regulates mDia2-initiated filopodial length, dynamics, and function. *Mol Biol Cell* **25**, 2604-2619 (2014).

16. J. Block *et al.*, Filopodia formation induced by active mDia2/Drf3. *J Microsc* **231**, 506-517 (2008).

17. S. Pellegrin, H. Mellor, The Rho family GTPase Rif induces filopodia through mDia2. *Curr Biol* **15**, 129-133 (2005).

18. J. Block *et al.*, FMNL2 drives actin-based protrusion and migration downstream of Cdc42. *Curr Biol* **22**, 1005-1012 (2012).

19. E. S. Harris, T. J. Gauvin, E. G. Heimsath, H. N. Higgs, Assembly of filopodia by the formin FRL2 (FMNL3). *Cytoskeleton (Hoboken)* **67**, 755-772 (2010).

20. L. E. Young, E. G. Heimsath, H. N. Higgs, Cell type-dependent mechanisms for formin-mediated assembly of filopodia. *Mol Biol Cell* **26**, 4646-4659 (2015).

21. D. A. Applewhite *et al.*, Ena/VASP proteins have an anti-capping independent function in filopodia formation. *Mol Biol Cell* **18**, 2579-2591 (2007).

22. A. Schirenbeck, R. Arasada, T. Bretschneider, M. Schleicher, J. Faix, Formins and VASPs may co-operate in the formation of filopodia. *Biochem Soc Trans* **33**, 1256-1259 (2005).

23. M. L. Kerber, R. E. Cheney, Myosin-X: a MyTH-FERM myosin at the tips of filopodia. *J Cell Sci* **124**, 3733-3741 (2011).

24. A. D. Sousa, R. E. Cheney, Myosin-X: a molecular motor at the cell's fingertips. *Trends Cell Biol* **15**, 533-539 (2005).

25. H. Zhang *et al.*, Myosin-X provides a motor-based link between integrins and the cytoskeleton. *Nat Cell Biol* **6**, 523-531 (2004).

26. B. Hoffmann, C. Schafer, Filopodial focal complexes direct adhesion and force generation towards filopodia outgrowth. *Cell Adh Migr* **4**, 190-193 (2010).

27. F. Lagarrigue *et al.*, A RIAM/lamellipodin-talin-integrin complex forms the tip of sticky fingers that guide cell migration. *Nat Commun* **6**, 8492 (2015).

28. C. Schafer *et al.*, One step ahead: role of filopodia in adhesion formation during cell migration of keratinocytes. *Exp Cell Res* **315**, 1212-1224 (2009).

29. C. Schafer *et al.*, The key feature for early migratory processes: Dependence of adhesion, actin bundles, force generation and transmission on filopodia. *Cell Adh Migr* **4**, 215-225 (2010).

30. B. Geiger, J. P. Spatz, A. D. Bershadsky, Environmental sensing through focal adhesions. *Nat Rev Mol Cell Biol* **10**, 21-33 (2009).

31. Z. Sun, S. S. Guo, R. Fassler, Integrin-mediated mechanotransduction. *J Cell Biol* **215**, 445-456 (2016).

32. D. Riveline *et al.*, Focal contacts as mechanosensors: externally applied local mechanical force induces growth of focal contacts by an mDia1-dependent and ROCK-independent mechanism. *J Cell Biol* **153**, 1175-1186 (2001).

33. J. M. Goffin *et al.*, Focal adhesion size controls tension-dependent recruitment of alpha-smooth muscle actin to stress fibers. *J Cell Biol* **172**, 259-268 (2006).

34. M. Prager-Khoutorsky *et al.*, Fibroblast polarization is a matrix-rigidity-dependent process controlled by focal adhesion mechanosensing. *Nat Cell Biol* **13**, 1457-1465 (2011).

35. L. Trichet *et al.*, Evidence of a large-scale mechanosensing mechanism for cellular adaptation to substrate stiffness. *Proc Natl Acad Sci U S A* **109**, 6933-6938 (2012).

36. S. Wong, W. H. Guo, Y. L. Wang, Fibroblasts probe substrate rigidity with filopodia extensions before occupying an area. *Proc Natl Acad Sci U S A* **111**, 17176-17181 (2014).

37. J. S. Berg, R. E. Cheney, Myosin-X is an unconventional myosin that undergoes intrafilopodial motility. *Nat Cell Biol* **4**, 246-250 (2002).

38. T. M. Watanabe, H. Tokuo, K. Gonda, H. Higuchi, M. Ikebe, Myosin-X induces filopodia by multiple elongation mechanism. *J Biol Chem* **285**, 19605-19614 (2010).

39. R. C. Smith *et al.*, Regulation of myosin filament assembly by light-chain phosphorylation. *Philos Trans R Soc Lond B Biol Sci* **302**, 73-82 (1983).

40. V. Betapudi, Life without double-headed non-muscle myosin II motor proteins. *Front Chem* **2**, 45 (2014).

41. M. Vicente-Manzanares, X. Ma, R. S. Adelstein, A. R. Horwitz, Non-muscle myosin II takes centre stage in cell adhesion and migration. *Nat Rev Mol Cell Biol* **10**, 778-790 (2009).

42. S. Hu *et al.*, Long-range self-organization of cytoskeletal myosin II filament stacks. *Nat Cell Biol* **19**, 133-141 (2017).

43. S. A. Rizvi *et al.*, Identification and characterization of a small molecule inhibitor of formin-mediated actin assembly. *Chem Biol* **16**, 1158-1168 (2009).

44. H. Tokuo, M. Ikebe, Myosin X transports Mena/VASP to the tip of filopodia. *Biochem Biophys Res Commun* **319**, 214-220 (2004).

45. C. H. Yu, J. B. Law, M. Suryana, H. Y. Low, M. P. Sheetz, Early integrin binding to Arg-Gly-Asp peptide activates actin polymerization and. *Proc Natl Acad Sci U S A* **108**, 20585-20590 (2011).

46. N. Billington, A. Wang, J. Mao, R. S. Adelstein, J. R. Sellers, Characterization of three full-length human nonmuscle myosin II paralogs. *J Biol Chem* **288**, 33398-33410 (2013).

47. N. Hundt, W. Steffen, S. Pathan-Chhatbar, M. H. Taft, D. J. Manstein, Load-dependent modulation of non-muscle myosin-2A function by tropomyosin 4.2. *Sci Rep* **6**, 20554 (2016).

48. M. Kovacs, F. Wang, A. Hu, Y. Zhang, J. R. Sellers, Functional divergence of human cytoplasmic myosin II: kinetic characterization of the non-muscle IIA isoform. *J Biol Chem* **278**, 38132-38140 (2003).

49. J. Yan, M. Yao, B. T. Goult, M. P. Sheetz, Talin Dependent Mechanosensitivity of Cell Focal Adhesions. *Cell Mol Bioeng* **8**, 151-159 (2015).

50. P. Atherton *et al.*, Vinculin controls talin engagement with the actomyosin machinery. *Nat Commun* **6**, 10038 (2015).

51. X. Hu *et al.*, Cooperative Vinculin Binding to Talin Mapped by Time-Resolved Super Resolution Microscopy. *Nano Lett* **16**, 4062-4068 (2016).

52. W. Hu, B. Wehrle-Haller, V. Vogel, Maturation of filopodia shaft adhesions is upregulated by local cycles of. *PLoS One* **9**, 0107097 (2014).

53. B. T. Goult *et al.*, RIAM and vinculin binding to talin are mutually exclusive and regulate adhesion. *J Biol Chem* **288**, 8238-8249 (2013).

54. E. M. Lafuente *et al.*, RIAM, an Ena/VASP and Profilin ligand, interacts with Rap1-GTP and mediates Rap1-induced adhesion. *Dev Cell* **7**, 585-595 (2004).

55. N. Courtemanche, J. Y. Lee, T. D. Pollard, E. C. Greene, Tension modulates actin filament polymerization mediated by formin and profilin. *Proc Natl Acad Sci U S A* **110**, 9752-9757 (2013).

56. A. Jegou, M. F. Carlier, G. Romet-Lemonne, Formin mDia1 senses and generates mechanical forces on actin filaments. *Nat Commun* **4**, 1883 (2013).

57. M. M. Kozlov, A. D. Bershadsky, Processive capping by formin suggests a force-driven mechanism of actin polymerization. *J Cell Biol* **167**, 1011-1017 (2004).

58. M. Yu *et al.*, mDia1 senses both force and torque during F-actin filament polymerization. *In submission*, (2017).

59. C. G. Galbraith, K. M. Yamada, J. A. Galbraith, Polymerizing actin fibers position integrins primed to probe for adhesion sites. *Science* **315**, 992-995 (2007).

60. C. E. Chan, D. J. Odde, Traction dynamics of filopodia on compliant substrates. *Science* **322**, 1687-1691 (2008).

61. C. M. Lo, H. B. Wang, M. Dembo, Y. L. Wang, Cell movement is guided by the rigidity of the substrate. *Biophys J* **79**, 144-152 (2000).

62. S. R. Heidemann, D. Bray, Tension-driven axon assembly: a possible mechanism. *Front Cell Neurosci* **9**, 316 (2015).

63. P. C. Kerstein, R. I. Nichol, T. M. Gomez, Mechanochemical regulation of growth cone motility. *Front Cell Neurosci* **9**, 244 (2015).

64. P. C. Bridgman, S. Dave, C. F. Asnes, A. N. Tullio, R. S. Adelstein, Myosin IIB is required for growth cone motility. *J Neurosci* **21**, 6159-6169 (2001).

65. D. Bray, Mechanical tension produced by nerve cells in tissue culture. *J Cell Sci* **37**, 391-410 (1979).

66. M. Bai, B. Harfe, P. Freimuth, Mutations that alter an Arg-Gly-Asp (RGD) sequence in the adenovirus type 2 penton base protein abolish its cell-rounding activity and delay virus reproduction in flat cells. *J Virol* **67**, 5198-5205 (1993).

67. Y. Paran *et al.*, Development and application of automatic high-resolution light microscopy for cell-based screens. *Methods Enzymol* **414**, 228-247 (2006).

68. M. J. Schell, C. Erneux, R. F. Irvine, Inositol 1,4,5-trisphosphate 3-kinase A associates with F-actin and dendritic spines via its N terminus. *J Biol Chem* **276**, 37537-37546 (2001).

69. A. Kengyel, W. A. Wolf, R. L. Chisholm, J. R. Sellers, Nonmuscle myosin IIA with a GFP fused to the N-terminus of the regulatory light chain is regulated normally. *J Muscle Res Cell Motil* **31**, 163-170 (2010).

70. A. Y. Lin, E. Prochniewicz, Z. M. James, B. Svensson, D. D. Thomas, Large-scale opening of utrophin's tandem calponin homology (CH) domains upon actin binding by an induced-fit mechanism. *Proc Natl Acad Sci U S A* **108**, 12729-12733 (2011).

71. S. J. Winder *et al.*, Calmodulin regulation of utrophin actin binding. *Biochem Soc Trans* **23**, 397S (1995).

72. S. Watanabe *et al.*, mDia2 induces the actin scaffold for the contractile ring and stabilizes its position during cytokinesis in NIH 3T3 cells. *Mol Biol Cell* **19**, 2328-2338 (2008).

73. R. Brock, T. M. Jovin, Heterogeneity of signal transduction at the subcellular level: microsphere-based focal EGF receptor activation and stimulation of Shc translocation. *J Cell Sci* **114**, 2437-2447 (2001).

74. K. C. Neuman, S. M. Block, Optical trapping. *Rev Sci Instrum* **75**, 2787-2809 (2004).

75. M. A. Toth *et al.*, Biochemical Activities of the Wiskott-Aldrich Syndrome Homology Region 2 Domains of Sarcomere Length Short (SALS) Protein. *J Biol Chem* **291**, 667-680 (2016).

76. J. A. Spudich, S. Watt, The regulation of rabbit skeletal muscle contraction. I. Biochemical studies of the interaction of the tropomyosin-troponin complex with actin and the proteolytic fragments of myosin. *J Biol Chem* **246**, 4866-4871 (1971).

77. S. Romero *et al.*, Formin is a processive motor that requires profilin to accelerate actin assembly and associated ATP hydrolysis. *Cell* **119**, 419-429 (2004).

78. D. Tsygankov *et al.*, CellGeo: a computational platform for the analysis of shape changes in cells with complex geometries. *J Cell Biol* **204**, 443-460 (2014).

79. W. C. Lin, C. H. Yu, S. Triffo, J. T. Groves, Supported membrane formation, characterization, functionalization, and patterning. *Curr Protoc Chem Biol* **2**, 235-269 (2010).

80. J. Gelles, B. J. Schnapp, M. P. Sheetz, Tracking kinesin-driven movements with nanometre-scale precision. *Nature* **331**, 450-453 (1988).

Acknowledgments: Encouraging and stimulating discussions with Drs. D. Bray (University of Cambrige, UK), M.M. Kozlov (Tel Aviv University, Israel) are much appreciated. We are grateful to Dr. T. Kachanawong (MBI, Singapore) for providing genetic constructs, Dr. D. Kovar (University of Chicago, IL, USA) for a sample of SMIFH2 inhibitor, and Dr. Tsygankov (Georgia Tech, USA) for providing code for filopodia length computation. We thank the Protein Cloning and Expression Core facility of the MBI for help with sub-cloning of mCherry-mDia2 and mApple-myosin X. We also thank Dr. F. Margadant and Lau Wai Han (MBI Microscopy Core facility) and Dr. V. Vyasnoff (MBI, Singapore) for their kind help with the optical tweezers setup. This research has been supported by the National Research Foundation Singapore, Ministry of Education of Singapore, Grant R714006006271 & R714019006271 (awarded to A.D.B.), Grant MOE2012T31001 (awarded to Y.J.) and BMRC Grant A*Star-JST 1514324022 (awarded to A.D.B.). As well we thank S. Wolf and A. Wang (Science Communication MBI, Singapore) for excellent editorial help.

Figure 1

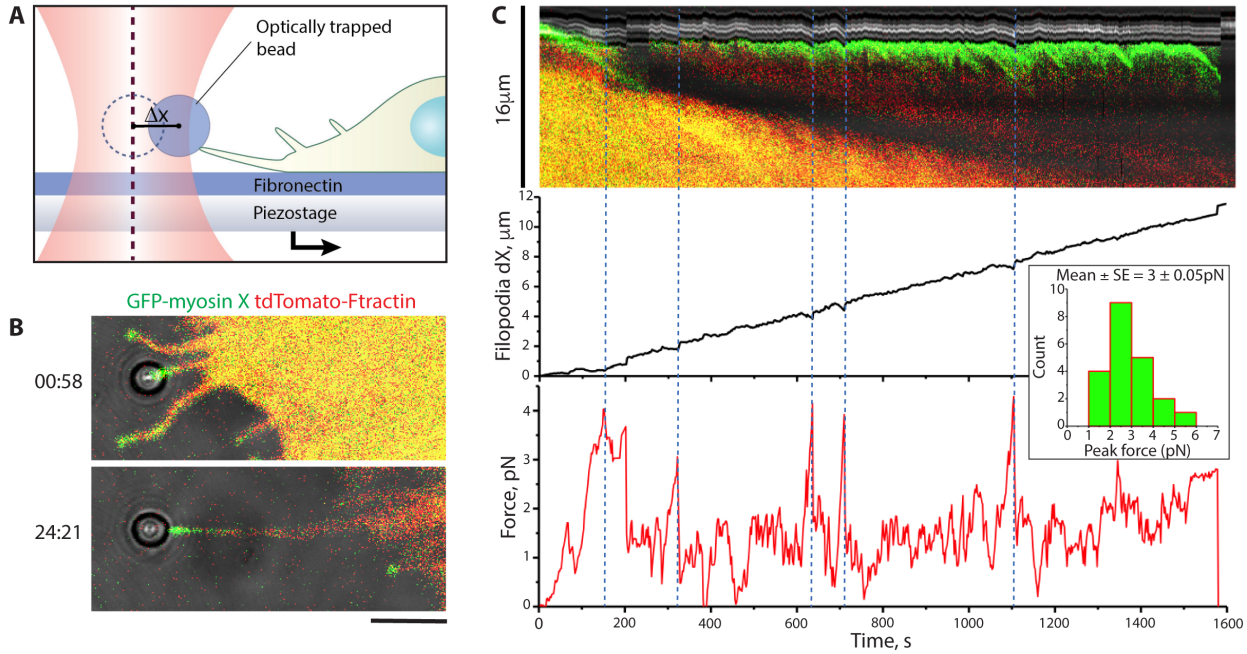
A
Optically trapped bead
ΔX
Fibronectin
Piezostage
B
GFP-myosin X tdTomato-Ftractin
00:58
24:21
C
16μm
Filopodia dX, μm
Mean ± SE = 3 ± 0.05pN
Count
Peak force (pN)
Force, pN
Time, s

Fig. 1. Dynamics of pulling-induced filopodia growth

(A) Experimental setup used to observe force-induced filopodia growth. Optical tweezers was used to trap fibronectin-coated microbeads attached to filopodia tips. **(B)** Images of a typical cell expressing GFP-myosin X and tdTomato-Ftractin with an attached bead, taken immediately after starting of stage movement (top) and in the course of sustained growth (bottom). Note that both myosin X and actin remain at the filopodium tip during growth. **(C)** Top panel: A kymograph showing the dynamics of myosin X and actin in the filopodium shown in (B). Middle panel: Filopodium growth in relation to the coordinate system of the microscope stage. The origin of the coordinate system corresponds to the bead position in the center of the laser trap at the initial time point. The coordinate of the bead is changing due to the uniform movement of the stage, and fluctuations of the bead position inside the trap. Lower panel: Forces experienced by the bead. Note the discrete peak force values correspond to the moments of filopodia growth cessation (seen in the middle panel) as marked with dotted lines. Inset: The distribution of peak force values, based on the pooled measurements of 21 peaks from 8 beads in 6 independent experiments. Scale bar, 5μm.

Figure 2

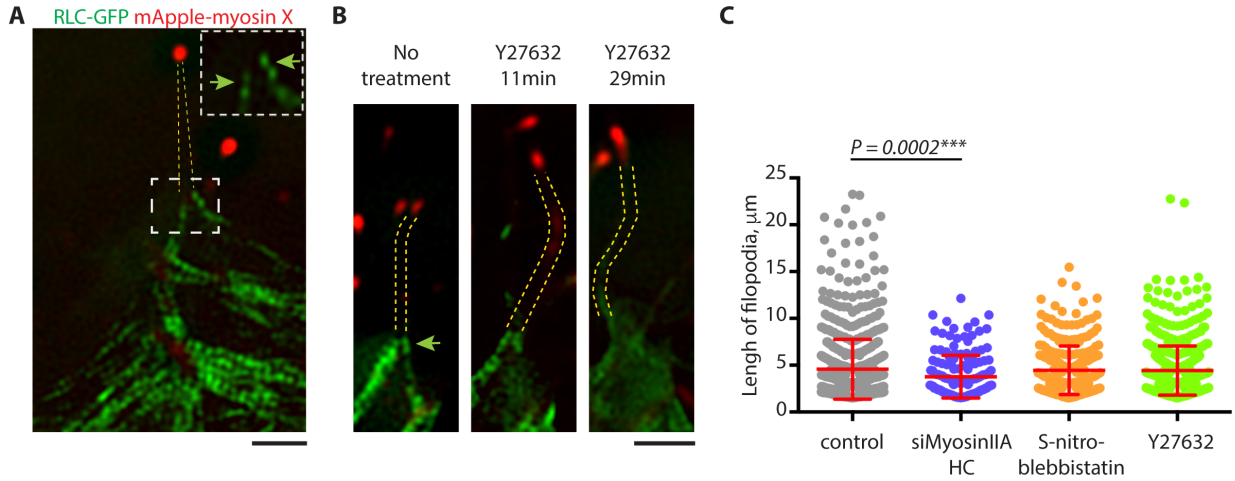
A
RLC-GFP mApple-myosin X
B
No treatment
Y27632 11min
Y27632 29min
C
P = 0.0002***
Lengh of filopodia, µm
25
20
15
10
5
0
control
siMyosinIIA HC
S-nitro-blebbistatin
Y27632

Fig. 2. Myosin II filaments at the base of filopodia

(A) Structured illumination microscopy (SIM) visualization of myosin II (RLC-GFP, green) and mApple-myosin X (red). Note myosin X at the filopodium tip and 2 bipolar myosin II filaments at the filopodium base (boxed area). Myosin II filaments are seen as doublets of fluorescent spots, which correspond to the myosin II heads (arrows in the inset). **(B)** Myosin II filaments gradually disappear following cell treatment with Y27632 (30μM). Images of the same filopodium, taken at different times, following inhibitor addition are shown. Filopodia contours in (A) and (B) are marked by dashed lines. **(C)** Distributions and average lengths of free filopodia (those not attached to beads) in control cells, and cells with myosin II function impaired by different treatments. Symbols correspond to individual filopodia. The mean values are indicated by thick horizontal red lines; the error bars correspond to SDs. The mean lengths of control GFP-myosin X induced filopodia, and filopodia from myosin II siRNA, S-nitro-blebbistatin (20μM, 1hour), and Y27632 (30μM, 1 hour) treated cells, were (mean±SEM) 4.6±0.1μm (n = 922, 38 cells), 3.8±0.2μm (n = 160, 18 cells), 4.5±0.1μm (n = 299, 24 cells), 4.4±0.1μm (n = 656, 27 cells), respectively. Scale bars, 2μm.

Figure 3

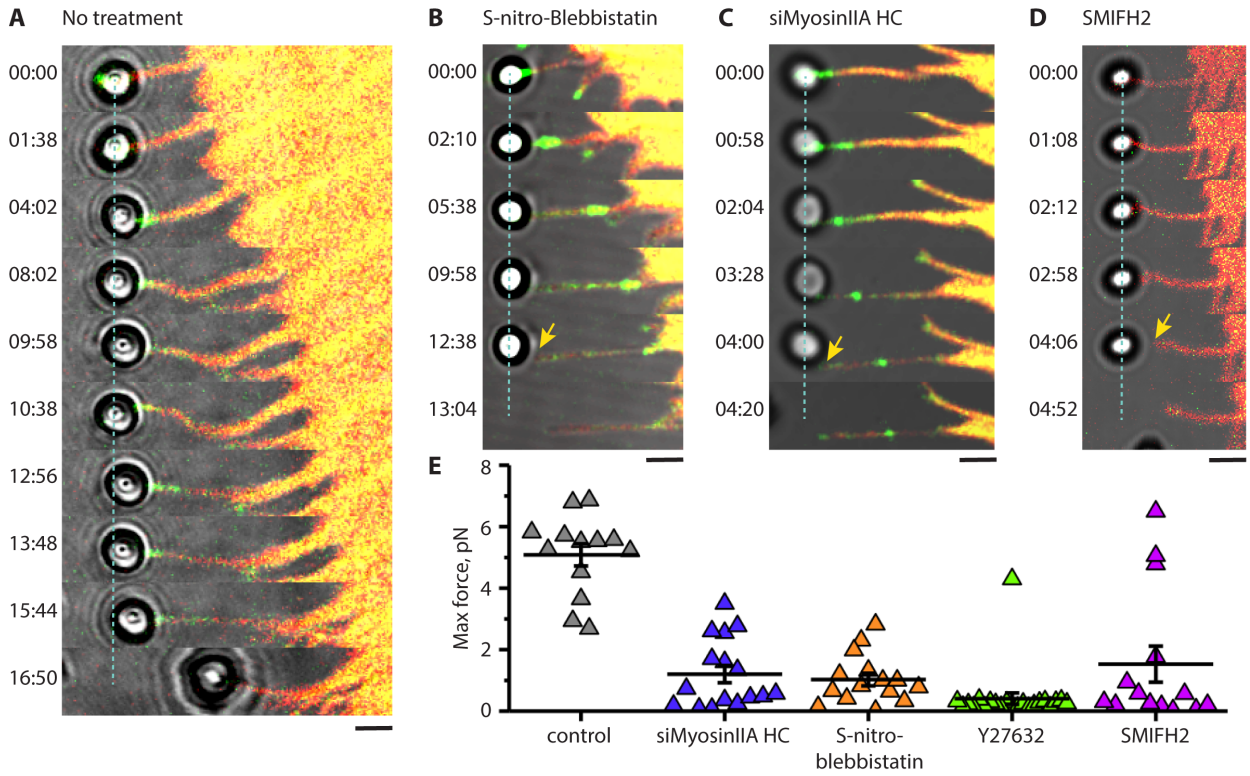
A
No treatment
00:00
01:38
04:02
08:02
09:58
10:38
12:56
13:48
15:44
16:50
B
S-nitro-Blebbistatin
00:00
02:10
05:38
09:58
12:38
13:04
C
siMyosinIIA HC
00:00
00:58
02:04
03:28
04:00
04:20
D
SMIFH2
00:00
01:08
02:12
02:58
04:06
04:52
E
Max force, pN
0
2
4
6
8
control
siMyosinIIA HC
S-nitro-blebbistatin
Y27632
SMIFH2

Fig. 3. Inhibition of myosin II or formin reduces filopodia adhesion

(A) Filopodium growth upon application of pulling force. The deflection of the bead from its initial position at the center of the laser trap (dashed line) is proportional to the forces exerted by the filopodium (see Fig. 1). At 16:50 min the filopodium retracted and pulled the bead out of the trap. **(B-D)** Filopodia in cells with suppressed myosin II activity cannot maintain sustained adhesion to the bead and do not produce forces sufficient for noticeable bead deflection during the stage movement. Cells treated with 20μM of S-nitro-blebbistatin for 10-20 min (B), transfected with myosin IIA siRNA (C), or treated for 1 hour with 40μM of the formin inhibitor SMIFH2 (D) are shown. Yellow arrows indicate the filopodia detachment from the beads. GFP-myosin X (green) and tdTomato-Ftractin (red) are labeled. Scale bars, 2μm. (**E**) Peak values of the forces exerted by filopodia on the beads during the stage movement in control cells (no treatment) and in cells transfected with myosin IIA siRNA, or treated with S-nitro-blebbistatin, Y27632 (30μM, 10-20 min), or SMIFH2. Mean values (horizontal lines) and SEMs (error bars) are indicated. The mean±SEM of the maximal forces exerted by control filopodia (5.1±0.4pN, n = 13) was significantly higher than those in myosin IIA knockdown, as well as S-nitro-blebbistatin-, Y27632-, and SMIFH2-treated cells (1.2±0.3, n = 16; 1.0±0.2, n = 15; 0.4±0.2, n = 22; and 1.5±0.6pN, n = 14, respectively) ($p<0.0001$ for control vs all treatment cases).

Figure 4

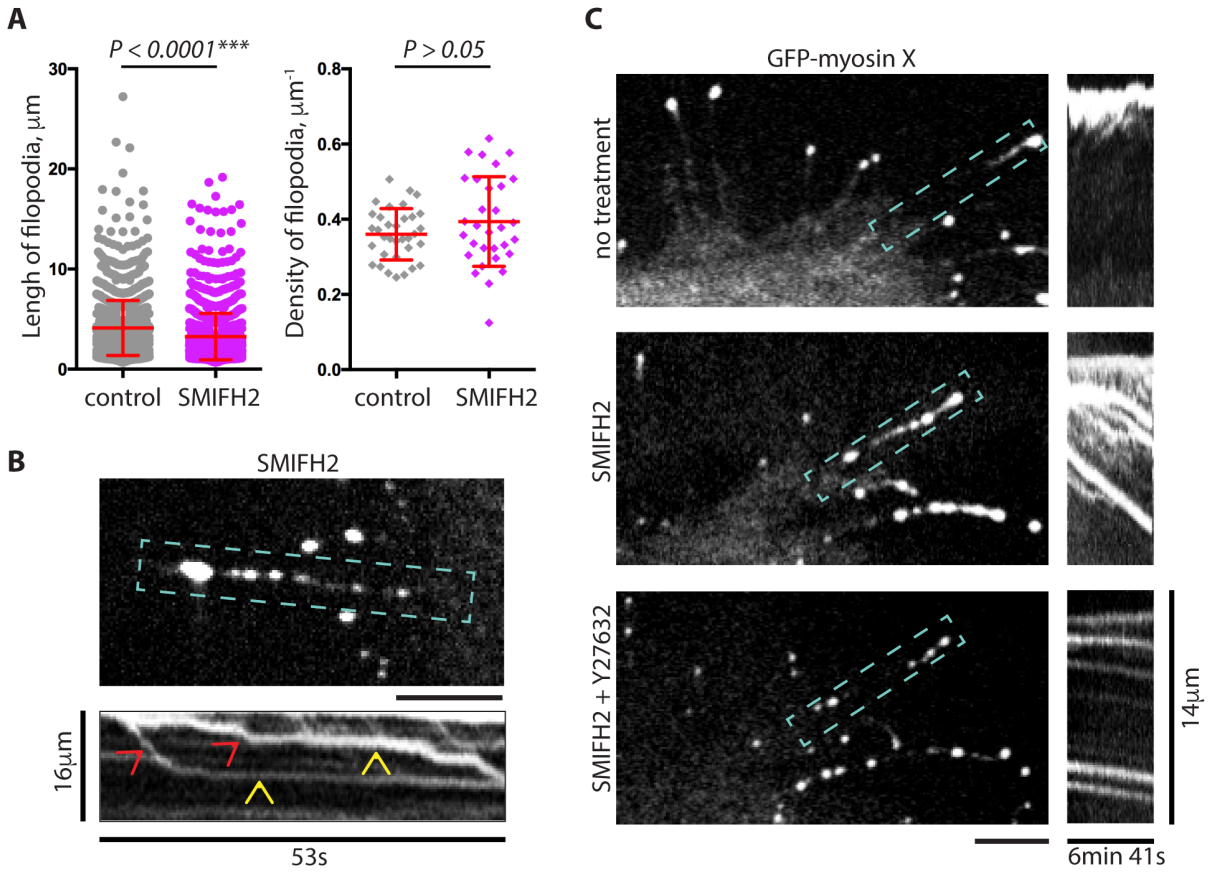
A
P < 0.0001***
Lengh of filopodia, µm
30
20
10
0
control
SMIFH2
P > 0.05
Density of filopodia, µm-1
0.8
0.6
0.4
0.2
0.0
control
SMIFH2
B
SMIFH2
16µm
53s
C
GFP-myosin X
no treatment
SMIFH2
SMIFH2 + Y27632
14µm
6min 41s

Fig. 4. Effect of formin inhibition on filopodia growth and centripetal movement of myosin X patches

(A) The length of unconstrained filopodia in control cells expressing GFP-myosin X 4.1±0.1μm (n = 1710 in 34 cells) (mean±SEM) exceeded that of SMIFH2 treated cells 3.2±0.1μm (n = 1645 in 31 cells), while the numbers of filopodia per micron of cell boundary did not differ significantly: 0.36±0.01 (n = 34 cells) and 0.39±0.02 (n = 31 cells) (mean±SEM). **(B)** Upper panel: disintegration of the myosin X comet tail following a 2 hours exposure to 20μM SMIFH2, numerous myosin X patches are seen in the filopodia shaft. Lower panel: a kymograph showing fast centripetal movement of the patches boxed in the upper panel towards the cell body (red arrowheads, see also movie S4). Intervals of constitutive slow centripetal movements are indicated by yellow arrowheads. **(C)** Y27632 treatment stopped the movement of myosin X patches in SMIFH2 treated cells. The same filopodium is shown before SMIFH2 treatment (upper panel), 15 min after the addition of 20μM SMIFH2 (middle panel) and 15 min after subsequent addition of 30μM Y27632 (lower panel). Myosin X patches are shown in the left images (see also movies S5A-C), and kymographs representing the movement of the patches in the boxed area - in the images on the right. Scale bars, 5μm.

Figure 5

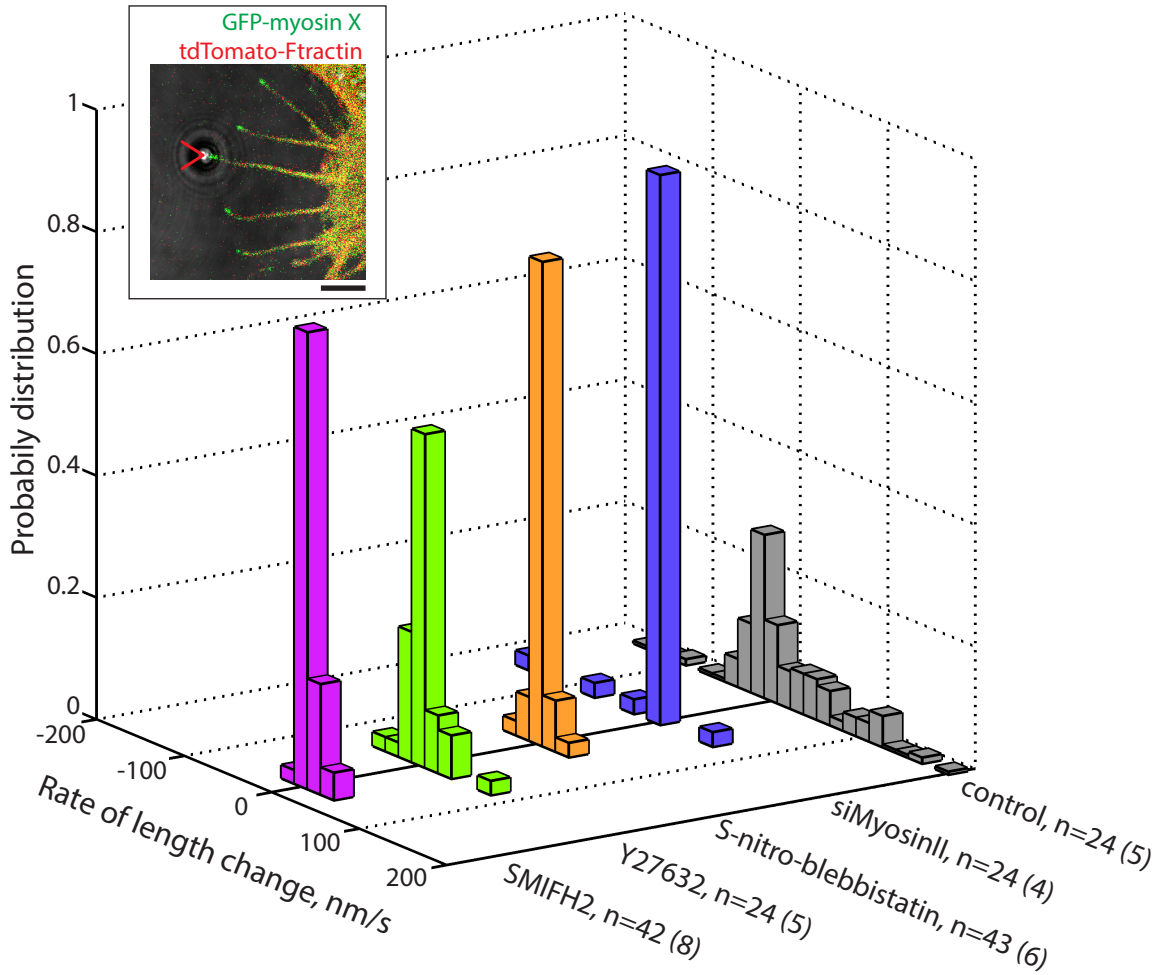
GFP-myosin X
tdTomato-Ftractin
Probabily distribution
1
0.8
0.6
0.4
0.2
0
-200
-100
0
100
200
Rate of length change, nm/s
SMIFH2, n=42 (8)
Y27632, n=24 (5)
S-nitro-blebbistatin, n=43 (6)
siMyosinII, n=24 (4)
control, n=24 (5)

Fig. 5. Inhibition of myosin II or formins interfere with growth of unconstrained filopodia

A graph showing the distribution of growth/retraction velocities of unconstrained filopodia for control, myosin II siRNA knockdown, S-nitro-blebbistatin, Y27632 and SMIFH2 treatment, observed in the same experiments as those assessing bead attached filopodia. n represents the number of filopodia (with number of cells in parenthesis). (Inset) A cell expressing GFP-myosin X and tdTomato-Ftractin, which is representative of those used in experiments assessing filopodia growth. The filopodium attached to the laser trapped fibronectin-coated bead is indicated by red arrowhead. Such filopodia were excluded from the score. Scale bar, 5μm.

Figure 6

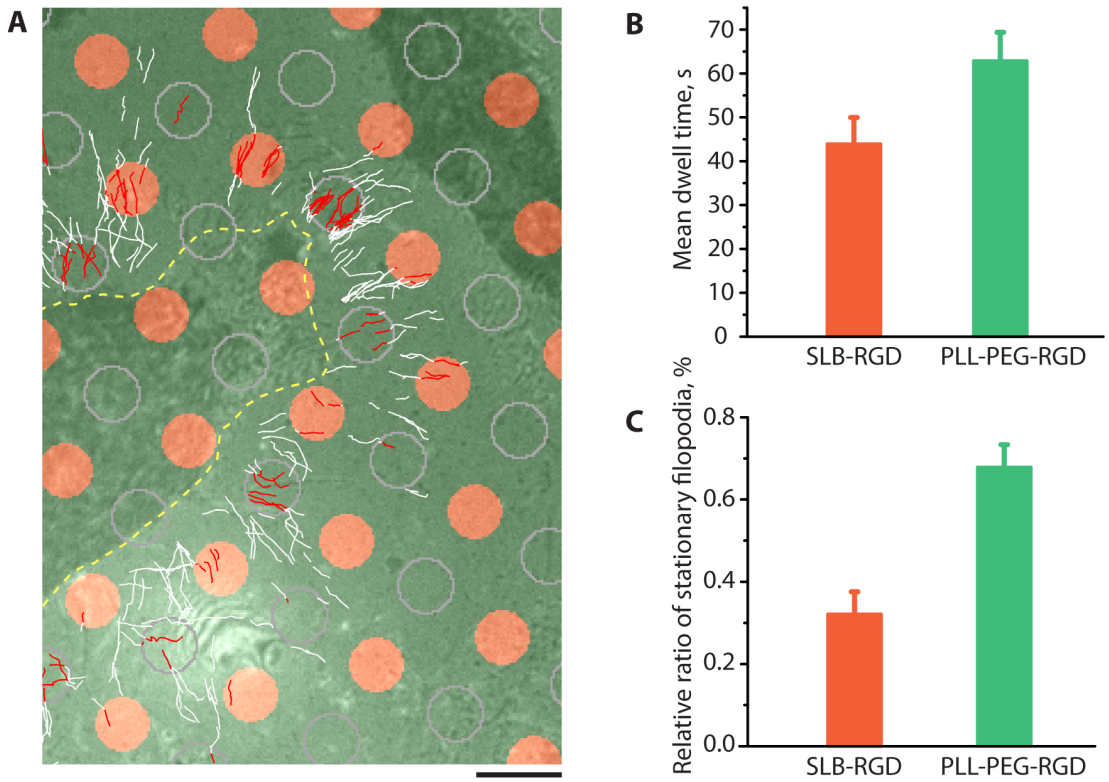
A
B
Mean dwell time, s
70
60
50
40
30
20
10
0
SLB-RGD
PLL-PEG-RGD
C
Relative ratio of stationary filopodia, %
0.8
0.6
0.4
0.2
0.0
SLB-RGD
PLL-PEG-RGD

Fig. 6. Attachment of filopodia to RGD-coated rigid and fluid substrate

(A) The cells expressing GFP-myosin X were plated on micropatterned coverslips covered with circular islands (D = 3μm) of supported lipid bilayer (SLB) conjugated to RGD (orange circles), organized into a square lattice. The glass between the islands was covered with poly-L-lysine-PEG conjugated to RGD at the same density (Fig. S8). Trajectories of GFP-positive filopodia tips acquired during a 14-36 min time interval are shown. The cell border is shown by a yellow dashed line. For comparison of the trajectories on rigid and fluid substrates, the circles of similar diameter were drawn by computer in the centers of the square lattice formed by SLB islands (outlined by gray contours). The segments of the trajectories located inside either the SLB islands or the drawn circles on the rigid substrate are shown in red, and the remaining parts of the trajectories are shown in white. Scale bar, 5μm. **(B-C)** Quantification of the trajectories of filopodia tips inside rigid and fluid circular islands for five cells (at least 200 individual trajectories per cell were scored). **(B)** The bars represent the average dwelling time that filopodia tips spent inside rigid (turquoise) or fluid (red) circles defined above. **(C)** Fraction of filopodia tip trajectories remaining inside rigid circles (green bar) and fluid circles (orange bar) relatively to the total number of trajectories in the circles during the period of observation. Error bars correspond to the SEM.

Supplementary Materials

Materials and Methods

Figs. S1 to S8

Captions for Figs. S1 to S8

Captions for Movies S1 to S9

Movies S1 to S9

1. Jacquemet, G., Hamidi, H. & Ivaska, J. Filopodia in cell adhesion, 3D migration and cancer cell invasion. *Curr Opin Cell Biol* **36**, 23-31 (2015).
2. Mattila, P.K. & Lappalainen, P. Filopodia: molecular architecture and cellular functions. *Nat Rev Mol Cell Biol* **9**, 446-454 (2008).
3. Heckman, C.A. & Plummer, H.K., 3rd Filopodia as sensors. *Cell Signal* **25**, 2298-2311 (2013).
4. Bryant, P.J. Filopodia: fickle fingers of cell fate? *Curr Biol* **9**, R655-657 (1999).
5. Prols, F., Sagar & Scaal, M. Signaling filopodia in vertebrate embryonic development. *Cell Mol Life Sci* **73**, 961-974 (2016).
6. Romero, S. *et al.* Filopodium retraction is controlled by adhesion to its tip. *J Cell Sci* **125**, 4999-5004 (2012).
7. Vonna, L., Wiedemann, A., Aepfelbacher, M. & Sackmann, E. Micromechanics of filopodia mediated capture of pathogens by macrophages. *Eur Biophys J* **36**, 145-151 (2007).
8. Moller, J., Luhmann, T., Chabria, M., Hall, H. & Vogel, V. Macrophages lift off surface-bound bacteria using a filopodium-lamellipodium hook-and-shovel mechanism. *Sci Rep* **3**, 2884 (2013).
9. Bornschlogl, T. *et al.* Filopodial retraction force is generated by cortical actin dynamics and controlled by reversible tethering at the tip. *Proc Natl Acad Sci U S A* **110**, 18928-18933 (2013).
10. Faix, J., Breitsprecher, D., Stradal, T.E. & Rottner, K. Filopodia: Complex models for simple rods. *Int J Biochem Cell Biol* **41**, 1656-1664 (2009).
11. Jaiswal, R. *et al.* The formin Daam1 and fascin directly collaborate to promote filopodia formation. *Curr Biol* **23**, 1373-1379 (2013).
12. Vignjevic, D. *et al.* Role of fascin in filopodial protrusion. *J Cell Biol* **174**, 863-875 (2006).
13. Delanote, V. *et al.* An alpaca single-domain antibody blocks filopodia formation by obstructing L-plastin-mediated F-actin bundling. *FASEB J* **24**, 105-118 (2010).
14. Van Audenhove, I. *et al.* Fascin Rigidity and L-plastin Flexibility Cooperate in Cancer Cell Invadopodia and Filopodia. *J Biol Chem* **291**, 9148-9160 (2016).
15. Barzik, M., McClain, L.M., Gupton, S.L. & Gertler, F.B. Ena/VASP regulates mDia2-initiated filopodial length, dynamics, and function. *Mol Biol Cell* **25**, 2604-2619 (2014).
16. Block, J. *et al.* Filopodia formation induced by active mDia2/Drf3. *J Microsc* **231**, 506-517 (2008).
17. Pellegrin, S. & Mellor, H. The Rho family GTPase Rif induces filopodia through mDia2. *Curr Biol* **15**, 129-133 (2005).
18. Block, J. *et al.* FMNL2 drives actin-based protrusion and migration downstream of Cdc42. *Curr Biol* **22**, 1005-1012 (2012).
19. Harris, E.S., Gauvin, T.J., Heimsath, E.G. & Higgs, H.N. Assembly of filopodia by the formin FRL2 (FMNL3). *Cytoskeleton (Hoboken)* **67**, 755-772 (2010).
20. Young, L.E., Heimsath, E.G. & Higgs, H.N. Cell type-dependent mechanisms for formin-mediated assembly of filopodia. *Mol Biol Cell* **26**, 4646-4659 (2015).
21. Applewhite, D.A. *et al.* Ena/VASP proteins have an anti-capping independent function in filopodia formation. *Mol Biol Cell* **18**, 2579-2591 (2007).
22. Schirenbeck, A., Arasada, R., Bretschneider, T., Schleicher, M. & Faix, J. Formins and VASPs may co-operate in the formation of filopodia. *Biochem Soc Trans* **33**, 1256-1259 (2005).
23. Kerber, M.L. & Cheney, R.E. Myosin-X: a MyTH-FERM myosin at the tips of filopodia. *J Cell Sci* **124**, 3733-3741 (2011).
24. Sousa, A.D. & Cheney, R.E. Myosin-X: a molecular motor at the cell's fingertips. *Trends Cell Biol* **15**, 533-539 (2005).
25. Zhang, H. *et al.* Myosin-X provides a motor-based link between integrins and the cytoskeleton. *Nat Cell Biol* **6**, 523-531 (2004).
26. Hoffmann, B. & Schafer, C. Filopodial focal complexes direct adhesion and force generation towards filopodia outgrowth. *Cell Adh Migr* **4**, 190-193 (2010).
27. Lagarrigue, F. *et al.* A RIAM/lamellipodin-talin-integrin complex forms the tip of sticky fingers that guide cell migration. *Nat Commun* **6**, 8492 (2015).
28. Schafer, C. *et al.* One step ahead: role of filopodia in adhesion formation during cell migration of keratinocytes. *Exp Cell Res* **315**, 1212-1224 (2009).
29. Schafer, C. *et al.* The key feature for early migratory processes: Dependence of adhesion, actin bundles, force generation and transmission on filopodia. *Cell Adh Migr* **4**, 215-225 (2010).

30. Geiger, B., Spatz, J.P. & Bershadsky, A.D. Environmental sensing through focal adhesions. *Nat Rev Mol Cell Biol* **10**, 21-33 (2009).
31. Sun, Z., Guo, S.S. & Fassler, R. Integrin-mediated mechanotransduction. *J Cell Biol* **215**, 445-456 (2016).
32. Riveline, D. *et al.* Focal contacts as mechanosensors: externally applied local mechanical force induces growth of focal contacts by an mDia1-dependent and ROCK-independent mechanism. *J Cell Biol* **153**, 1175-1186 (2001).
33. Goffin, J.M. *et al.* Focal adhesion size controls tension-dependent recruitment of alpha-smooth muscle actin to stress fibers. *J Cell Biol* **172**, 259-268 (2006).
34. Prager-Khoutorsky, M. *et al.* Fibroblast polarization is a matrix-rigidity-dependent process controlled by focal adhesion mechanosensing. *Nat Cell Biol* **13**, 1457-1465 (2011).
35. Trichet, L. *et al.* Evidence of a large-scale mechanosensing mechanism for cellular adaptation to substrate stiffness. *Proc Natl Acad Sci U S A* **109**, 6933-6938 (2012).
36. Wong, S., Guo, W.H. & Wang, Y.L. Fibroblasts probe substrate rigidity with filopodia extensions before occupying an area. *Proc Natl Acad Sci U S A* **111**, 17176-17181 (2014).
37. Berg, J.S. & Cheney, R.E. Myosin-X is an unconventional myosin that undergoes intrafilopodial motility. *Nat Cell Biol* **4**, 246-250 (2002).
38. Watanabe, T.M., Tokuo, H., Gonda, K., Higuchi, H. & Ikebe, M. Myosin-X induces filopodia by multiple elongation mechanism. *J Biol Chem* **285**, 19605-19614 (2010).
39. Smith, R.C. *et al.* Regulation of myosin filament assembly by light-chain phosphorylation. *Philos Trans R Soc Lond B Biol Sci* **302**, 73-82 (1983).
40. Betapudi, V. Life without double-headed non-muscle myosin II motor proteins. *Front Chem* **2**, 45 (2014).
41. Vicente-Manzanares, M., Ma, X., Adelstein, R.S. & Horwitz, A.R. Non-muscle myosin II takes centre stage in cell adhesion and migration. *Nat Rev Mol Cell Biol* **10**, 778-790 (2009).
42. Hu, S. *et al.* Long-range self-organization of cytoskeletal myosin II filament stacks. *Nat Cell Biol* **19**, 133-141 (2017).
43. Rizvi, S.A. *et al.* Identification and characterization of a small molecule inhibitor of formin-mediated actin assembly. *Chem Biol* **16**, 1158-1168 (2009).
44. Tokuo, H. & Ikebe, M. Myosin X transports Mena/VASP to the tip of filopodia. *Biochem Biophys Res Commun* **319**, 214-220 (2004).
45. Yu, C.H., Law, J.B., Suryana, M., Low, H.Y. & Sheetz, M.P. Early integrin binding to Arg-Gly-Asp peptide activates actin polymerization and. *Proc Natl Acad Sci U S A* **108**, 20585-20590 (2011).
46. Billington, N., Wang, A., Mao, J., Adelstein, R.S. & Sellers, J.R. Characterization of three full-length human nonmuscle myosin II paralogs. *J Biol Chem* **288**, 33398-33410 (2013).
47. Hundt, N., Steffen, W., Pathan-Chhatbar, S., Taft, M.H. & Manstein, D.J. Load-dependent modulation of non-muscle myosin-2A function by tropomyosin 4.2. *Sci Rep* **6**, 20554 (2016).
48. Kovacs, M., Wang, F., Hu, A., Zhang, Y. & Sellers, J.R. Functional divergence of human cytoplasmic myosin II: kinetic characterization of the non-muscle IIA isoform. *J Biol Chem* **278**, 38132-38140 (2003).
49. Yan, J., Yao, M., Goult, B.T. & Sheetz, M.P. Talin Dependent Mechanosensitivity of Cell Focal Adhesions. *Cell Mol Bioeng* **8**, 151-159 (2015).
50. Atherton, P. *et al.* Vinculin controls talin engagement with the actomyosin machinery. *Nat Commun* **6**, 10038 (2015).
51. Hu, X. *et al.* Cooperative Vinculin Binding to Talin Mapped by Time-Resolved Super Resolution Microscopy. *Nano Lett* **16**, 4062-4068 (2016).
52. Hu, W., Wehrle-Haller, B. & Vogel, V. Maturation of filopodia shaft adhesions is upregulated by local cycles of. *PLoS One* **9**, 0107097 (2014).
53. Goult, B.T. *et al.* RIAM and vinculin binding to talin are mutually exclusive and regulate adhesion. *J Biol Chem* **288**, 8238-8249 (2013).
54. Lafuente, E.M. *et al.* RIAM, an Ena/VASP and Profilin ligand, interacts with Rap1-GTP and mediates Rap1-induced adhesion. *Dev Cell* **7**, 585-595 (2004).
55. Courtemanche, N., Lee, J.Y., Pollard, T.D. & Greene, E.C. Tension modulates actin filament polymerization mediated by formin and profilin. *Proc Natl Acad Sci U S A* **110**, 9752-9757 (2013).
56. Jegou, A., Carlier, M.F. & Romet-Lemonne, G. Formin mDia1 senses and generates mechanical forces on actin filaments. *Nat Commun* **4**, 1883 (2013).
57. Kozlov, M.M. & Bershadsky, A.D. Processive capping by formin suggests a force-driven mechanism of actin polymerization. *J Cell Biol* **167**, 1011-1017 (2004).

58. Yu, M. *et al.* mDia1 senses both force and torque during F-actin filament polymerization. *In submission* (2017).
59. Galbraith, C.G., Yamada, K.M. & Galbraith, J.A. Polymerizing actin fibers position integrins primed to probe for adhesion sites. *Science* **315**, 992-995 (2007).
60. Chan, C.E. & Odde, D.J. Traction dynamics of filopodia on compliant substrates. *Science* **322**, 1687-1691 (2008).
61. Lo, C.M., Wang, H.B., Dembo, M. & Wang, Y.L. Cell movement is guided by the rigidity of the substrate. *Biophys J* **79**, 144-152 (2000).
62. Heidemann, S.R. & Bray, D. Tension-driven axon assembly: a possible mechanism. *Front Cell Neurosci* **9**, 316 (2015).
63. Kerstein, P.C., Nichol, R.I. & Gomez, T.M. Mechanochemical regulation of growth cone motility. *Front Cell Neurosci* **9**, 244 (2015).
64. Bridgman, P.C., Dave, S., Asnes, C.F., Tullio, A.N. & Adelstein, R.S. Myosin IIB is required for growth cone motility. *J Neurosci* **21**, 6159-6169 (2001).
65. Bray, D. Mechanical tension produced by nerve cells in tissue culture. *J Cell Sci* **37**, 391-410 (1979).